

# Acetaldehyde as a probe for the chemical properties of aluminophosphate molecular sieves. An in situ FT-IR study

Mi Suk Jeong<sup>1</sup>, Heinz Frei<sup>\*</sup>

*Physical Biosciences Division, Calvin Laboratory, Lawrence Berkeley National Laboratory, University of California, Berkeley, CA 94720, USA*

Received 26 August 1999; received in revised form 1 October 1999; accepted 5 November 1999

## Abstract

Loading of acetaldehyde from the gas phase into transition metal substituted aluminophosphate sieves of AFI structure resulted in mainly physisorbed  $\text{CH}_3\text{CH}=\text{O}$  in the case of  $\text{FeAlPO}_4\text{-5}$ . By contrast, FT-IR spectroscopy revealed extensive chemical reaction upon loading into metal-free  $\text{AlPO}_4\text{-5}$  and  $\text{CoAlPO}_4\text{-5}$  materials at temperatures as low as  $-100^\circ\text{C}$ . The low temperature product is identified as acetaldol, which dehydrates to crotonaldehyde upon warm-up to room temperature. The reactive sites are proposed to be Lewis acid sites in the aluminophosphate framework. Using FT-IR monitoring of acetaldehyde in the pores of aluminophosphate sieves as a sensitive method for the detection of Lewis acid sites, we find that their abundance varies substantially with metal substitution. Interestingly, isomorphous Fe substitution of the aluminophosphate framework seems to suppress the formation of such defect sites. © 2000 Elsevier Science B.V. All rights reserved.

*Keywords:* Aluminophosphate molecular sieve; Transition metals; Infrared spectroscopy; Acetaldehyde; Lewis acid sites

## 1. Introduction

Aluminophosphate molecular sieves containing isomorphically substituted transition metals in the framework [1–3] have great potential for application in catalysis. Most applications have thus far centered on liquid phase hydrocarbon oxidations over metal substituted aluminophosphates [4–6]. Equally interesting use of these materials can be envisioned in light-driven redox chemistry, an aspect that remains to be explored. Framework transition metals can act

as robust chromophores and redox centers, furnishing opportunities for UV or visible light-induced electron transfer chemistry of gaseous or liquid reactants adsorbed onto the sieve. Progress in these areas depends on mechanistic understanding of these catalysts, especially the nature of the active sites.

Study of the structural changes of small probe molecules adsorbed on solid surfaces by infrared spectroscopy is a well established method for identifying and characterizing catalytic sites. Framework metals may specifically interact with molecules adsorbed at the gas–micropore interface, and frequencies may be sensitive to the oxidation state of the metal. In addition, acid sites, basic sites or defects on the pore surface

<sup>\*</sup> Corresponding author.

<sup>1</sup> Present address: Department of Chemistry and Biochemistry, Utah State University, Logan, UT 84322, USA.

may induce chemical reaction. Acetaldehyde has been used as an effective probe in zeolites [7–10] and on silica or silica-supported metal catalysts [11,12], for example. In this paper, we communicate an FT-IR study of acetaldehyde adsorbed on type AFI aluminophosphate molecular sieves  $\text{AlPO}_4\text{-5}$ ,  $\text{CoAlPO}_4\text{-5}$ , and  $\text{FeAlPO}_4\text{-5}$  [2,3]. In these materials, metals occupy framework sites with tetrahedral coordination [13]. Spectra and chemical changes of the adsorbed molecule were monitored in the temperature range 170 to 300 K. Based on infrared analysis of the observed structural changes and processes, the probable nature of the sites that activate acetaldehyde inside the micropores is discussed.

## 2. Experimental

Aluminophosphate molecular sieves of type  $\text{AlPO}_4\text{-5}$  and  $\text{CoAlPO}_4\text{-5}$  were synthesized from gels with molecular composition  $\text{Et}_3\text{N} \cdot \text{Al}_2\text{O}_3 \cdot \text{P}_2\text{O}_5 \cdot 40\text{H}_2\text{O}$  or  $\text{Et}_3\text{N} \cdot \text{Al}_2\text{O}_3 \cdot \text{P}_2\text{O}_5 \cdot 0.04\text{CoO} \cdot 40\text{H}_2\text{O}$ , respectively, in an autoclave under autogeneous pressure at 175°C for 24 h. The aluminophosphate sources for the AFI samples were pseudo-boehmite (Catapal, 72%  $\text{Al}_2\text{O}_3$ , Vista), phosphoric acid (Fluka, 85%), and triethylamine (Fluka). As cobalt source,  $\text{Co(II)} (\text{CH}_3\text{CO}_2)_2 \cdot 4\text{H}_2\text{O}$  (Fluka) was used. Framework substitution of Co was determined to be  $\text{Co}/(\text{Al} + \text{P}) = 0.01$ . A sample of  $\text{FeAlPO}_4\text{-5}$  was kindly prepared in our laboratory by Dr. N. Ulagappan. All materials were synthesized using modifications of procedures described in the literature [14]. Powder XRD patterns showed the as-synthesized material to be highly crystalline and pure. All samples were calcined at 550°C in flowing oxygen overnight to remove the organic template. During calcination, as-synthesized  $\text{CoAlPO}_4\text{-5}$  turned from deep blue to green. Treatment of the calcined  $\text{CoAlPO}_4\text{-5}$  with a flow of a  $\text{H}_2/\text{N}_2$  mixture (10%  $\text{H}_2$ ) at 400°C for 3 h reversed the green color to deep blue. This is taken as evidence for tetrahedral

coordination of the Co centers in the framework and for reversible change of oxidation state between  $\text{Co}^{+II}$  and  $\text{Co}^{+III}$  by some groups [15], although interconversion between distorted tetrahedral  $\text{Co}^{+II}$  sites has also been proposed [3,16]. Samples reduced by an alternative route, namely slurring of the calcined powder in methanol at room temperature followed by washing with distilled water and drying at 120°C, were also used.

Diffuse reflectance UV–Vis spectra were recorded in the region 240–800 nm using a Shimadzu spectrometer Model 2100 with an integrating sphere Model ISR-260, with  $\text{BaSO}_4$  as reference. In situ FT-IR spectroscopy of acetaldehyde adsorbed on  $\text{CoAlPO}_4\text{-5}$ ,  $\text{FeAlPO}_4\text{-5}$ , and  $\text{AlPO}_4\text{-5}$  was conducted with an IBM-Bruker Model IFS 113 instrument. Self-supporting pressed wafers of approx. 10 mg weight were placed in a miniature infrared vacuum cell mounted inside a variable temperature vacuum system (Oxford Model Optistat). The temperature was tunable from 77 to 473 K. Prior to loading of acetaldehyde from the gas phase (approx. 6 Torr), the pellet was dehydrated at 200°C under high vacuum for 12–16 h (Varian turbomolecular pump Model V-60). Acetaldehyde (Aldrich, 99%), acetaldehyde- $^{13}\text{C}_2$  (Cambridge Isotope Laboratories, 99%  $^{13}\text{C}$ ), and crotonaldehyde (Aldrich, 99%) were used as received.

## 3. Results and discussion

### 3.1. Acetaldehyde adsorbed on $\text{FeAlPO}_4\text{-5}$

Aluminophosphate molecular sieves are transparent in the infrared region down to about  $1300\text{ cm}^{-1}$ . Below this region, framework stretching modes start to absorb. The only sharp feature of the dehydrated material is a weak band at  $3674\text{ cm}^{-1}$  originating from some framework P–OH groups [17]. The main infrared absorptions of  $\text{CH}_3\text{CH}=\text{O}$  gas adsorbed on  $\text{FeAlPO}_4\text{-5}$  molecular sieve are at 1352, 1398,

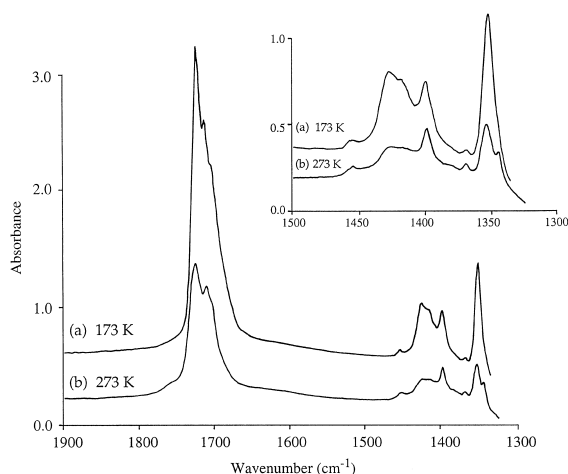


Fig. 1. Infrared spectra observed upon loading of 6 T  $\text{CH}_3\text{CH}=\text{O}$  gas into  $\text{FeAlPO}_4\text{-5}$  at 223 K. (a) Spectrum at 173 K; (b) after warm-up to 273 K.

1426, 1726, 2846, 2912, and 2996  $\text{cm}^{-1}$ . The fingerprint region of the spectrum recorded at 173 K (loading at 223 K), displayed in Fig. 1, trace (a), resembles closely that of  $\text{CH}_3\text{CH}=\text{O}$  loaded into zeolite CaY [18]. Hence, the main site of acetaldehyde in  $\text{FeAlPO}_4\text{-5}$  reflects non-specific adsorption without any distinct sign of interaction between guest molecule and Fe centers. There are several additional small peaks in the  $\text{CH}_3\text{CH}=\text{O}/\text{FeAlPO}_4\text{-5}$  spectrum which can be discerned from Fig. 1, namely at 1345, 1369, 1455, 1705 (shoulder), and 2940  $\text{cm}^{-1}$ . These bands, attributed to a species labeled P, do not change their intensity appreciably when raising the pellet temperature to 273 K. By contrast, all absorptions of acetaldehyde decrease by about a factor of three upon warm-up due to desorption of the molecule into the gas phase. This can readily be seen in trace (b) of Fig. 1. We conclude that P is a new species formed in trace amounts upon acetaldehyde adsorption into the sieve.

### 3.2. Acetaldehyde adsorbed on $\text{CoAlPO}_4\text{-5}$

Upon adsorption of acetaldehyde on  $\text{CoAlPO}_4\text{-5}$ , an infrared spectrum very different from that of  $\text{CH}_3\text{CH}=\text{O}$  on  $\text{FeAlPO}_4\text{-5}$  is ob-

served. Figs. 2 and 3 show the fingerprint region of the molecule adsorbed on calcined and reduced  $\text{CoAlPO}_4\text{-5}$ , respectively, at 173 K (trace (a)) and 273 K (trace (b)). Loading was again conducted at 223 K. In contrast to  $\text{CH}_3\text{CH}=\text{O}$  on  $\text{FeAlPO}_4\text{-5}$ , the species P bands dominate the fingerprint spectrum in the case of both calcined and reduced  $\text{CoAlPO}_4\text{-5}$  sieve. Frequencies of physisorbed acetaldehyde and of species P in calcined and reduced  $\text{CoAlPO}_4\text{-5}$  (using  $\text{H}_2$  or  $\text{CH}_3\text{OH}$ ) are essentially the same, and very close to those observed for  $\text{FeAlPO}_4\text{-5}$ . Observed bands are presented in Table 1 together with  $^{13}\text{C}$  isotope shifts and vibrational assignments. Aside from the more intense acetaldehyde spectrum in the case of calcined  $\text{CoAlPO}_4\text{-5}$  at 173 K compared to the reduced form (cf. intensities at 1417 and 1354  $\text{cm}^{-1}$  in

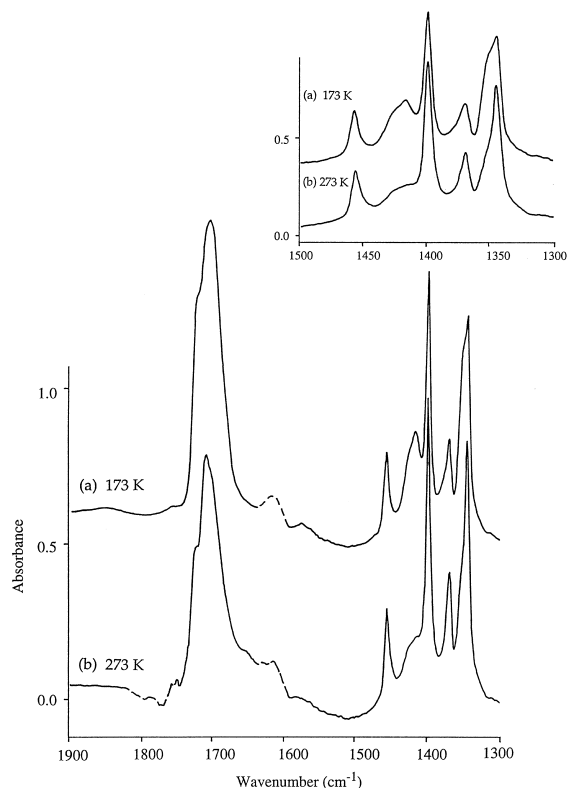


Fig. 2. Infrared spectra observed upon loading of  $\text{CH}_3\text{CH}=\text{O}$  into calcined  $\text{CoAlPO}_4\text{-5}$  at 223 K. (a) Spectrum at 173 K; (b) after warm-up to 273 K. Dotted features originate from residual  $\text{H}_2\text{O}$  or incomplete computer-subtraction of gas phase acetaldehyde.

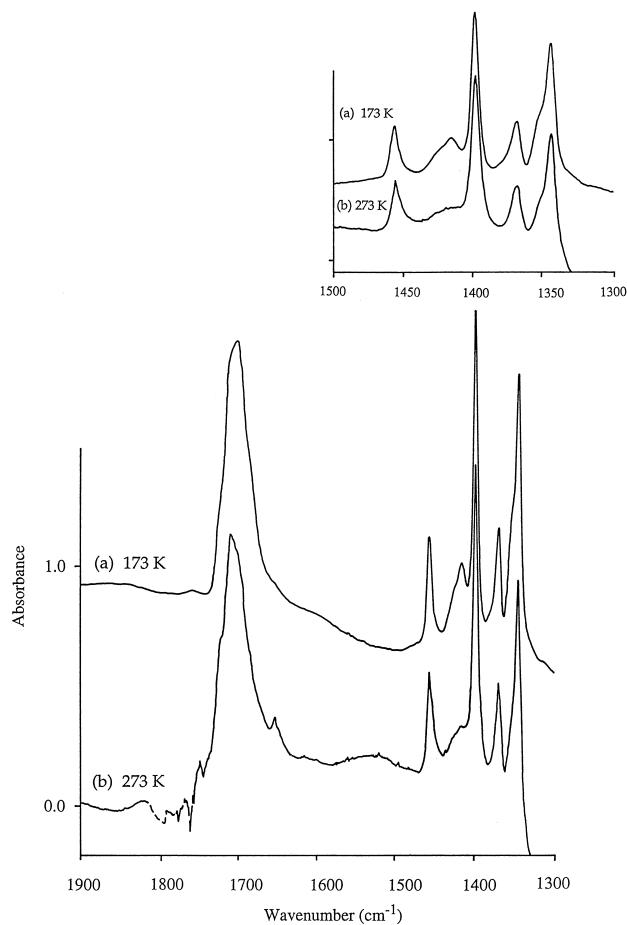


Fig. 3. Infrared spectra observed upon loading of  $\text{CH}_3\text{CH}=\text{O}$  into reduced ( $\text{H}_2$ )  $\text{CoAlPO}_4\text{-5}$  at 223 K. (a) Spectrum at 173 K; (b) after warm-up to 273 K.

Figs. 2a and 3a), no significant differences between these two samples are evident. The weak band at  $1653\text{ cm}^{-1}$  observed only in the 273 K spectra will be discussed below.

Fig. 4 shows electronic spectra in the region 240–800 nm of as-synthesized (a), calcined (b), and reduced (c)  $\text{CoAlPO}_4\text{-5}$  measured in the diffuse reflectance mode. The as-synthesized sample (trace (a)) shows absorption maxima at 538, 583, and 630 nm which are characteristic of a d–d electronic transition of tetrahedrally coordinated  $\text{Co}^{+II}(\text{d}^7)$  [20]. This indicates that, in this material, the dominant form of cobalt is lattice-substituted  $\text{Co}^{+II}$ , as has been reported by other groups [3,15]. Upon calcination, the intensity of the  $\text{Co}^{+II}$  transitions decreases while

a new absorption with shallow maxima at 325 and 413 nm grows in (trace (b)). It is generally attributed to a ligand-to-metal charge-transfer transition of  $\text{Co}^{+III}$  ions ( $\text{Co}^{+III}\text{-O}^{-II} \rightarrow \text{Co}^{+II}\text{-O}^{-I}$ ) formed upon oxidation of  $\text{Co}^{+II}$ . Previous studies have shown that only framework  $\text{Co}^{+II}$  is transformed to  $\text{Co}^{+III}$ , while any non-framework  $\text{Co}^{+II}$ , if present, is not oxidized [15]. EXAFS studies indicate that only a fraction, about 20%, of framework  $\text{Co}^{+II}$  is oxidized upon calcination [21]. Accordingly, framework  $\text{Co}^{+II}$  and  $\text{Co}^{+III}$  centers coexist in calcined  $\text{CoAlPO}_4\text{-5}$ . Trace (c) of Fig. 4 shows that when calcined  $\text{CoAlPO}_4\text{-5}$  was reduced with  $\text{H}_2$  gas, the 325 and 413 nm charge-transfer bands disappear completely under concurrent

Table 1  
Infrared spectrum upon adsorption of acetaldehyde on CoAPO-5<sup>a</sup>

Acetaldehyde			Species P		
Frequency, cm <sup>-1</sup>		Assignment <sup>b</sup>	Frequency, cm <sup>-1</sup>		Assignment
CH <sub>3</sub> CH=O	<sup>13</sup> CH <sub>3</sub> <sup>13</sup> CH=O shift		<sup>12</sup> C	<sup>13</sup> C shift	
1354	13	$\nu_7, \delta_s(\text{CH}_3)$	1345	10	$\delta(\text{CH})$
1399	0	$\nu_6, \delta(\text{CH})$	1368	3	$\delta_s(\text{CH}_3)$
1417	0	$\nu_5, \delta_{as}(\text{CH}_3)$	1399	16	$\delta(\text{COH})$ or $\nu(\text{CC}), \nu(\text{CO})$
1712	42	$\nu_4, \nu(\text{CO})$	1456	12	$\delta_{as}(\text{CH}_3)$
1728	42	$\nu_4, \nu(\text{CO})$	1705	40	$\nu(\text{CO})$
2731	8	$\nu_3, \nu(\text{CH})$ and 2 $\nu_6$ Fermi	2781	0	$\nu(\text{CH}) \nu(\text{CH}_3)$
2846	0	resonance	2846	0	$\nu(\text{CH}) \nu(\text{CH}_3)$
2912	0	$\nu_2, \nu_s(\text{CH}_3)$	2946	7	$\nu(\text{CH}) \nu(\text{CH}_3)$
2996	8	$\nu_{11}, \nu_{as}(\text{CH}_3)$	2996	8	$\nu(\text{CH}) \nu(\text{CH}_3)$

<sup>a</sup> $T = 173$  K, loading at 223 K. Frequencies for calcined and reduced CoAPO-5 are identical.

<sup>b</sup>Ref. [19].

increase of the visible Co<sup>2+</sup> (d–d) absorption at 528, 600, and 650 nm. This agrees with H<sub>2</sub>-reduced samples reported in the literature [15]. A similar spectrum was obtained upon reduction in a CH<sub>3</sub>OH slurry. While these observations point to a reversible oxidation and reduction of Co centers, an alternative interpretation in terms of Co<sup>2+</sup> in distorted tetrahedral environments based on ESR measurements has been presented [3,16]. However, since the change between calcined and reduced form of CoAlPO<sub>4</sub>-5 involves only about one-fifth of the metal centers, the

details of the Co state change do not affect the main conclusions of the acetaldehyde experiments reported here.

### 3.3. Acetaldehyde adsorbed on AlPO<sub>4</sub>-5

In order to determine whether species P produced on FeAlPO<sub>4</sub>-5 and CoAlPO<sub>4</sub>-5 is a result of acetaldehyde interaction with metal centers, we conducted infrared spectroscopic studies of the probe molecule adsorbed on AlPO<sub>4</sub>-5 sieve. As can readily be seen from Fig. 5, spectrum P is again more intense in the fingerprint region than that of acetaldehyde. Infrared band positions essentially coincide with those reported in Table 1 for CoAlPO<sub>4</sub>-5. Since no transition metal is present in the framework of AlPO<sub>4</sub>-5, we conclude that a site (or sites) associated with aluminum, phosphorous, or oxygen is responsible for the formation of P.

Infrared spectral changes observed upon warm-up of an AlPO<sub>4</sub>-5 pellet loaded with CH<sub>3</sub>CH=O from 173 to 243 K visualize the thermal interconversion of physisorbed acetaldehyde to P, as displayed in Fig. 6. The bands at 1724, 1711, 1417, and 1350 cm<sup>-1</sup> decrease by about a factor of 2 to 3. At the same time, growth of species P peaks is observed at 1456, 1399, 1369, and 1344 cm<sup>-1</sup>.

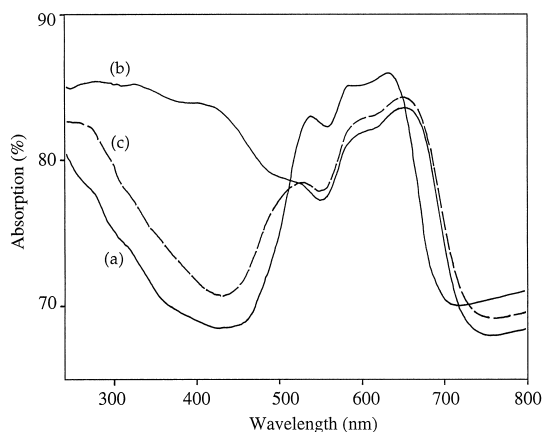


Fig. 4. UV-Vis reflectance spectra of CoAlPO<sub>4</sub>-5 molecular sieve. (a) As-synthesized sample; (b) after calcination; (c) after reduction of calcined sieve by H<sub>2</sub>.

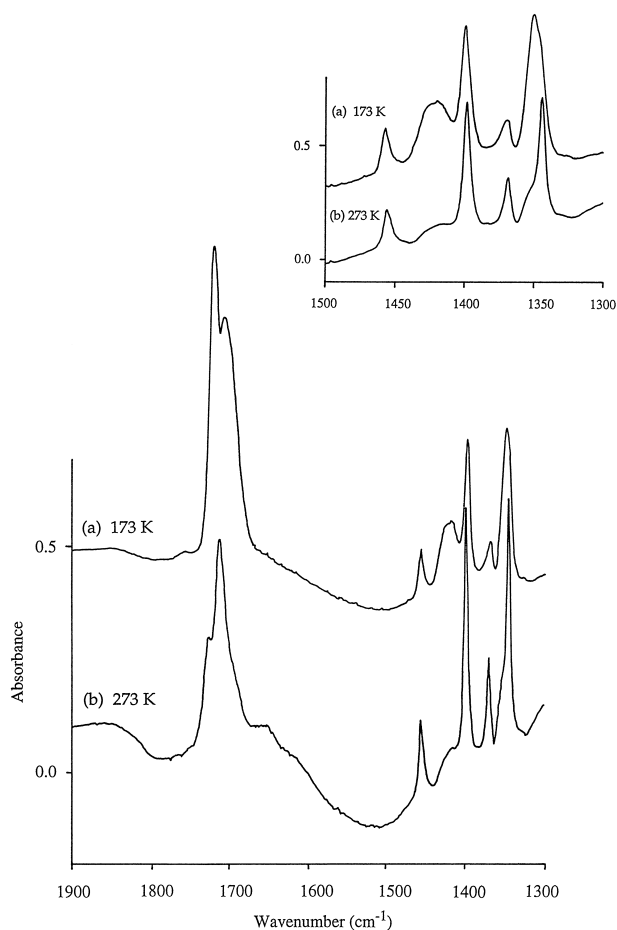


Fig. 5. Infrared spectra observed upon loading of  $\text{AlPO}_4\text{-5}$  at 223 K. (a) Spectrum at 173 K; (b) after warm-up to 273 K.

The  $1399\text{ cm}^{-1}$  band originates mainly from P, but  $\text{CH}_3\text{CH}=\text{O}$  contributes also. Similarly, the

low frequency part of the  $\text{C}=\text{O}$  stretch absorption decreases by less than a factor of two,

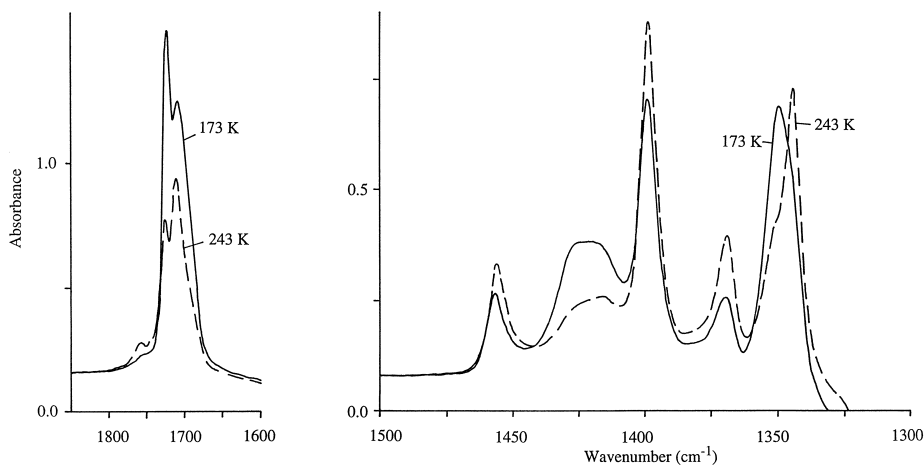


Fig. 6. Infrared spectra observed upon loading of  $\text{AlPO}_4\text{-5}$  at 223 K. The two traces were recorded at 173 K, and after warm-up to 243 K.

indicating growth of a species P band at 1705  $\text{cm}^{-1}$ .

### 3.4. Chemical reaction in $\text{AlPO}_4\text{-5}$ and $\text{CoAlPO}_4\text{-5}$ at room temperature

When loading  $\text{AlPO}_4\text{-5}$  or  $\text{CoAlPO}_4\text{-5}$  sieve (calcined or reduced) with acetaldehyde at room temperature (295 K), very little, if any, species P is formed. However, in addition to physisorbed  $\text{CH}_3\text{CH}=\text{O}$  bands, new, weak peaks could readily be detected at 1671 and 1653  $\text{cm}^{-1}$ . A spectrum of  $\text{CH}_3\text{CH}=\text{O}$  on reduced  $\text{CoAlPO}_4\text{-5}$  just after loading at 295 K is shown in Fig. 7a. Further spectral changes occurred within minutes, as can be seen from the difference spectra displayed in Fig. 7b. The acetaldehyde bands at 1712, 1417, and 1354  $\text{cm}^{-1}$

decrease under concurrent absorbance growth at 1672, 1653, 1620 (shoulder), 1445, 1393, 1377, and 1307  $\text{cm}^{-1}$ . Additional product peaks were noticed at 2975, 2936, and 2879  $\text{cm}^{-1}$ . All bands (except 1620  $\text{cm}^{-1}$ ) coincide with those of an authentic sample of crotonaldehyde in  $\text{CoAlPO}_4\text{-5}$ . The absorption at 1620  $\text{cm}^{-1}$  and a very broad feature centered around 3400  $\text{cm}^{-1}$  are attributed to  $\text{H}_2\text{O}$ , the co-product of aldol condensation.



Aside from crotonaldehyde and  $\text{H}_2\text{O}$ , no other product bands were observed. Relative intensities of product absorptions agreed well with those of the authentic crotonaldehyde spectrum. This allows us to conclude that, within 2% uncertainty, no higher condensation product was formed. Observations upon loading of  $\text{CH}_3\text{CH}=\text{O}$  in  $\text{AlPO}_4\text{-5}$  at 295 K were similar, indicating rapid crotonaldehyde formation as well. When  $\text{AlPO}_4$  or  $\text{CoAlPO}_4$  sieve loaded with  $\text{CH}_3\text{CH}=\text{O}$  was kept at low temperature to accumulate species P (Figs. 2, 3, 5) and then gradually warmed up, infrared difference spectra revealed interconversion of P to crotonaldehyde at temperatures above 0° C. We conclude that species P is an intermediate of aldol condensation of acetaldehyde to crotonaldehyde, most probably acetaldo [22].

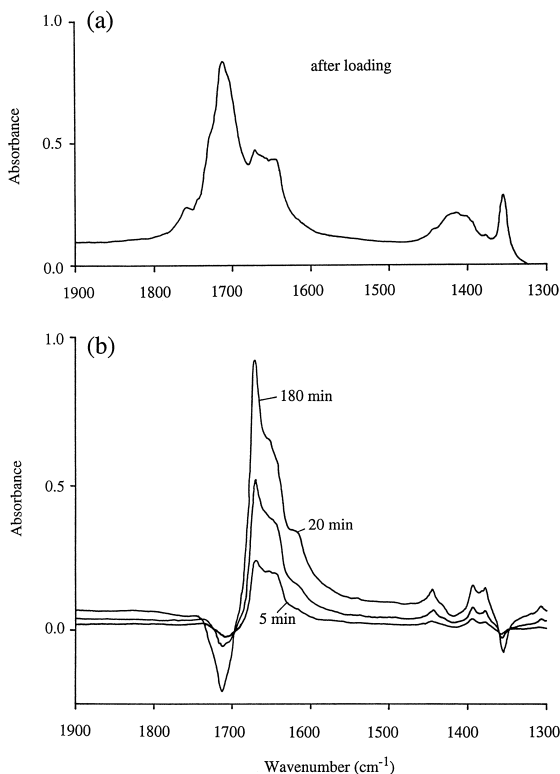
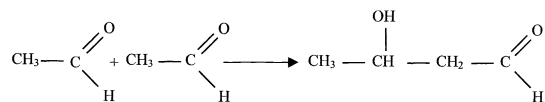
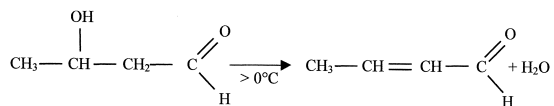


Fig. 7. Aldol condensation reaction in  $\text{CoAlPO}_4\text{-5}$  (reduced) at 295 K. (a) Spectrum just after loading of  $\text{CH}_3\text{CH}=\text{O}$  at 295 K; (b) infrared difference spectra recorded 5, 20, and 180 min after loading.



Indeed, the infrared bands of P (Table 1) agree well with the literature infrared spectrum of 3-hydroxybutanal [23]. The absence of a distinct OH stretch band of P around 3500  $\text{cm}^{-1}$  in the sieve is not surprising, as hydrogen bonding in the polar aluminosphosphate framework may render this band hundreds of  $\text{cm}^{-1}$  broad. Inter-

conversion of P to crotonaldehyde above 0°C reflects the spontaneous dehydration of the aldol intermediate.



By contrast to metal-free or Co substituted aluminophosphate sieve, no crotonaldehyde was detected upon loading of FeAlPO<sub>4</sub>-5 with acetaldehyde at 295 K. After 1 h, only minute growth of CH<sub>3</sub>–CH=CH–CH=O was indicated in this material by small peaks at 1670, 1650 and 1380 cm<sup>-1</sup>.

### 3.5. Catalytic sites

Aldol condensation of aldehydes is a well-established base catalyzed reaction in solution [22,24]. Acid catalyzed aldol reactions have also been reported [25], especially in zeolitic environments [10,26–30]. In the latter case, interaction of the carbonyl oxygen with Bronsted acid OH groups was proposed to activate acetaldehyde for aldol addition by rendering the carbonyl carbon more electrophilic [10,26]. IR spectra of our FeAlPO<sub>4</sub>, AlPO<sub>4</sub>, or CoAlPO<sub>4</sub>-5 materials did not reveal any Bronsted acid OH absorptions, which typically lie in the region between 3640 and 3580 cm<sup>-1</sup> [21]. Only the OH band of the weakly acidic P–OH groups at 3674 cm<sup>-1</sup> was observed whose intensity was the same within 20% in Co, Fe, and metal-free AlPO<sub>4</sub>-5 sieve. This is in agreement with previous infrared spectroscopic work on CoAlPO<sub>4</sub>-5 and AlPO<sub>4</sub>-5 [17,21]. Hence, neither Bronsted acid sites nor P–OH groups can be responsible for the observed aldol condensation. ESR active defect sites of the type recently reported by Hong et al. [31–33] for AlPO<sub>4</sub>-5 sieve are also unlikely to play a role. The concentration of these sites is orders of magnitude too low to account for aldol reaction at low temperature, where acetaldehyde is relatively immobile. On

the other hand, infrared [17,34] and EXAFS studies [21] revealed that CoAlPO<sub>4</sub>-5 in its calcined or reduced form possesses substantial concentrations (~0.1 mmol g<sup>-1</sup>) of Lewis acid sites. Barrett et al. [21] proposed that these sites are framework oxygen vacancies adjacent to Co<sup>+II</sup> centers. Such vacancies are expected to efficiently activate acetaldehyde molecules towards aldol addition by interacting with the carbonyl oxygen and thereby rendering the carbonyl carbon electrophilic, much like Lewis acid sites in steamed zeolite HY have been suggested to induce aldol condensation [35]. Our observation that, at 173K, the aldol adduct to acetaldehyde ratio is larger for reduced CoAlPO<sub>4</sub>-5 (Fig. 3) than the calcinated sieve (Fig. 2) is consistent with findings that the Lewis acid site concentration is higher in the reduced form [21,36]. Infrared spectroscopy of small nucleophilic molecules loaded into AlPO<sub>4</sub>-5 revealed similar concentrations of Lewis acid sites in the metal-free sieve [17]. We conclude that the most probable catalytic sites of aldol condensation are Lewis acid sites identified by previous X-ray absorption and infrared spectroscopic studies.

## 4. Conclusions

In-situ infrared monitoring of acetaldehyde gas loaded into AlPO<sub>4</sub>-5 sieve revealed aldol condensation at temperatures as low as –100°C by trapping of the acetaldol intermediate. The same transformation is observed to an even greater extent in framework-substituted CoAlPO<sub>4</sub>-5 and is attributed to activation of the aldehyde by Lewis acid sites. By contrast, very little aldol reaction takes place in Fe-substituted aluminophosphate sieve, which suggests that Lewis acid site concentrations in FeAlPO<sub>4</sub> are very small. This work shows that FT-IR spectroscopy of acetaldehyde offers a sensitive way of detecting Lewis acid sites in aluminophosphate sieves. The abundance of these sites varies strongly with metal substitution.



## Acknowledgements

This work was supported by the Director, Office of Science, Office of Basic Energy Sciences, Chemical Sciences Division of the U.S. Department of Energy under Contract No. DE-AC03-76SF00098. M.S.J. thanks the Korea Science and Engineering Foundation (KOSEF) for a fellowship.

## References

- [1] S.T. Wilson, B.M. Lok, C.A. Messina, T.R. Cannan, E.M. Flanigen, *J. Am. Chem. Soc.* 104 (1982) 1146.
- [2] S.T. Wilson, *Stud. Surf. Sci. Catal.* 58 (1991) 137.
- [3] M. Hartmann, L. Kevan, *Chem. Rev.* 99 (1999) 635.
- [4] R.A. Sheldon, *Stud. Surf. Sci. Catal.* 110 (1997) 151.
- [5] I.W.C.E. Arends, R.A. Sheldon, M. Wallace, V. Schuchardt, *Angew. Chem. Int. Ed. Engl.* 36 (1997) 1145.
- [6] R.A. Sheldon, *Top. Curr. Chem.* 164 (1993) 22.
- [7] C.D. Chavez-Diaz, S. Locatelli, E.E. Gonzo, *Zeolites* 12 (1992) 851.
- [8] J. Howard, J.M. Nicol, *J. Chem. Soc. Faraday Trans.* 86 (1990) 205.
- [9] K.T. Geodakyan, A.V. Kiselev, V.I. Lygin, *Russ. J. Phys. Chem.* 41 (1967) 476.
- [10] A.I. Biaglow, J. Sepa, R.J. Gorte, D. White, *J. Catal.* 151 (1995) 373.
- [11] D. Demri, J.P. Hindermann, C. Diagne, A. Kiennemann, *J. Chem. Soc. Faraday Trans.* 90 (1994) 501.
- [12] R.P. Young, N. Sheppard, *J. Catal.* 7 (1967) 223.
- [13] W.M. Meier, D.H. Olson, in: *Atlas of Zeolite Structure Types*, 4th edn., Elsevier, London, 1996, p. 26.
- [14] S.T. Wilson, E.M. Flanigen, *Eur. Pat.* 0132708, 1985.
- [15] A.A. Verberckmoes, M.G. Uytterhoeven, R.A. Schoonheydt, *Zeolites* 19 (1997) 180, and references therein.
- [16] V. Kurshev, L. Kevan, D.J. Parillo, C. Pereira, G.T. Kokotailo, R.J. Gorte, *J. Phys. Chem.* 98 (1994) 10160.
- [17] J. Janchen, M.P.J. Peeters, J.H.M.C. van Wolput, J.P. Wolthuisen, J.H.C. van Hooff, *J. Chem. Soc. Faraday Trans.* 90 (1994) 1033.
- [18] H. Sun, F. Blatter, H. Frei, *Catal. Lett.* 44 (1997) 247.
- [19] H. Hollenstein, Hs.H. Günthard, *Spectrochim. Acta* 27A (1971) 2027.
- [20] C. Montes, M.E. Davis, B. Murray, M. Narayana, *J. Phys. Chem.* 94 (1990) 6425.
- [21] P.A. Barrett, G. Sankar, C.R.A. Catlow, J.M. Thomas, *J. Phys. Chem.* 100 (1996) 8977.
- [22] J.D. Roberts, M.C. Caserio, in: *Basic Principles of Organic Chemistry*, Benjamin, New York, 1965, p. 479.
- [23] C.J. Pouchert, in: *The Aldrich Library of Infrared Spectra*, Aldrich, 1970, p. 218.
- [24] J. March, in: *Advanced Organic Chemistry*, 4th edn., Wiley, New York, 1992, p. 937.
- [25] W.T. Reichle, *J. Catal.* 63 (1980) 295.
- [26] P. Venuto, *Microporous Mater.* 2 (1994) 328.
- [27] R.J. Gorte, D. White, *Top. Catal.* 4 (1997) 57.
- [28] E.J. Munson, J.F. Haw, *Angew. Chem. Int. Ed. Engl.* 32 (1993) 615.
- [29] T. Xu, E.J. Munson, J.F. Haw, *J. Am. Chem. Soc.* 116 (1994) 1962.
- [30] V. Bosacek, L. Kubelkova, *Zeolites* 10 (1990) 64.
- [31] S.B. Hong, S.J. Kim, Y.S. Uh, *J. Am. Chem. Soc.* 118 (1996) 8102.
- [32] S.B. Hong, S.J. Kim, Y.S. Uh, *J. Phys. Chem.* 100 (1996) 15923.
- [33] S.J. Kim, M.H. Kim, S.B. Hong, Y.S. Uh, *Catal. Lett.* 44 (1997) 165.
- [34] M.P.J. Peeters, J.H.C. van Hooff, R.A. Sheldon, V.L. Zholobenko, L.M. Kustov, V.B. Kazansky, in: R. von Ballmoos, J.B. Higgins, M.M.J. Treacy (Eds.), *Proceedings of the 9th International Zeolite Conference*, Butterworth-Heinemann, Washington, DC, 1993, p. 651.
- [35] A.I. Biaglow, R.J. Gorte, D. White, *J. Catal.* 150 (1994) 221.
- [36] B. Kraushaar-Czarnetzki, W.G.M. Hoogervorst, R.R. Andrea, C.A. Emeis, W.H.J. Stork, *J. Chem. Soc. Faraday Trans.* 87 (1991) 891.